http://dx.doi.org/10.5012/bkcs.2014.35.1.189

White Light Emission from a Colloidal Mixture Containing ZnS Based Nanocrystals: ZnS, ZnS:Cu and ZnS:Mn

Jae Woog Lee and Cheong-Soo Hwang*

*Department of Chemistry, Institute of Nanosensor and Biotechnology, Center for Photofunctional Energy Materials (GRRC), Dankook University, Gyonggi-Do 448-701, Korea. *E-mail: cshwang@dankook.ac.kr*
Received August 27, 2013, Accepted October 28, 2013

Water dispersible ZnS based nanocrystals: ZnS (blue), ZnS:Cu (green) and ZnS:Mn (yellow-orange) were synthesized by capping the surface of the nanocrystals with a mercaptopropionic acid (MPA) molecule. The MPA capped ZnS based nanocrystal powders were characterized by using XRD, HR-TEM, EDXS, FT-IR, and FT-Raman spectroscopy. The optical properties of the colloidal nanocrystals were also measured by UV/Vis and photoluminescence (PL) spectroscopies in aqueous solvents. The PL spectra showed broad emission peaks at 440 nm (ZnS), 510 nm (ZnS:Cu) and 600 nm (ZnS:Mn), with relative PL efficiencies in the range of 4.38% to 7.20% compared to a reference organic dye. The measured average particle sizes from the HR-TEM images were in the range of 4.5 to 5.0 nm. White light emission was obtained by mixing these three nanocrystals at a molar ratio of 20 (ZnS):1 (ZnS:Cu):2 (ZnS:Mn) in water. The measured color coordinate of the white light was (0.31, 0.34) in the CIE chromaticity diagram, and the color temperature was 5527 K.

Key Words : ZnS, ZnS:Cu, ZnS:Mn nanocrystals, MPA capping, White light emission

Introduction

Semiconductor nanocrystals have gained great attention over the past decade.[1] These materials have widely applied in non-linear optics and electronic luminescence devices[2] and more recently in advanced biomedical area due to their unique physical, chemical and optical properties.[3] Most semiconductor nanocrystals show their unique size dependent optical properties resulted from the different band gap energies even between materials of identical chemical composition.[4,5] Zinc sulfide (ZnS) based semiconductor nanocrystals have attracted substantial interest due to their high quantum efficiencies and thermal stability at ambient temperature, which are critical properties for application in commercial electro-luminescence devices.[6] Many synthetic techniques used for such nanocrystals have been developed including gas, solid, and aqueous solution reactions *via* the thermal decomposition of organometallic precursors in hot organic solvents. However, these methods often require dangerously high temperatures and pressures, and even the use of highly bio-hazardous substances.[7-9] Especially, water dispersible semiconductor nanocrystals have been developed for fluorescent labeling agents used in advanced bio-imaging technology.[10,11] It was expected that these would replace the current complicated or hazardous radioactive disease detection techniques, and have formed the basis of very sensitive biological assays. In addition, such semiconducting nanocrystals are significantly more efficient, sensitive, and even thermally stable than the commercial organic dyes which are currently used in biomedical areas.[12] However, most semiconductor nanocrystals are synthesized in non-polar media, making them hardly compatible with any biological system; therefore, researchers needed to develop ways to solubilize the hydrophobic nanocrystals in water by modifying their surfaces.[13] For example, water-dispersible and bio-compatible ZnS:Mn nanocrystals capped their surfaces by conventional amino acids[14,15] and mercapto-acetic acid[16] has been synthesized and characterized in this laboratory. White light emitting semiconductor nanocrystals are important for use in various photoelectric devices such as solid state light emitting diodes (LEDs).[17] White light emission can be obtained by mixing complementary color emitting phosphors such as GaN (blue) and YAG:Ce (yellow).[18] Recent research regarding white light emitting nanocrystals have mainly focused on CdSe quantum dots which can emit both blue and yellow light by precisely controlling the particle sizes.[19] Previously in this lab, we reported the synthesis of white-light-emitting ZnSe:Mn nanocrystals formed by a thermal decomposition reaction of diethyl zinc, manganese(II) cyclohexabutylate, and elemental selenium dispersed in TOP solvent.[20] The obtained PL spectrum of ZnSe:Mn nanocrystals showed two broad emission peaks at 445 and 572 nm, and the resulting white light emission is produced by combining these complementary color emissions. In this article, we described the synthesis of three different color emitting ZnS based nanocrystals: ZnS (blue), ZnS:Cu (green), and ZnS:Mn (yellow-orange), simply by changing the dopant metal ions. Even though they are not perfectly complementary color combinations, we were able to obtain white-color emission by mixing the three nanophosphors at a proper ratio.

Experimental

Instrumentation. UV/Vis absorption spectra were recorded using a Perkin Elmer Lamda 25 spectrophotometer equipp-

ed with a deuterium/tungsten lamp. The FT-IR spectra were taken using a Perkin Elmer spectrophotometer equipped an attenuated total reflection (ATR) unit. The presented FT-Raman spectra were recorded by Bruker FRA106/s spectrophotometer with a resolution of 1 cm^{-1}. Solution photoluminescence spectra were taken by a Perkin Elmer LS-45 spectrophotometer equipped with a 500 W Xenon lamp, 0.275 m triple grating monochrometer, and PHV 400 photomultiplier tube. HR-TEM images were taken with a JEOL JEM 1210 electron microscope with a MAG mode of 1,000 to 800,000. The accelerating voltage was 40-120 kV. Samples for TEM were prepared *via* dispersion in methanol and placement on a carbon-coated copper grid (300 Mesh) followed by drying under vacuum. In addition, elemental compositions of the nanocrystals were determined by an Energy Dispersive X-ray Spectroscopy (EDXS) collecting unit equipped in the HR-TEM, with a Si (Li) detector in IXRF 500 system. ICP-AES elemental analyses were performed by Optima-430 (Perkin Elmer) spectrometer equipped with Echelle optics system and segmented array charge coupled device (SCD) detector. To prepare a sample of corresponding nanocrystal, a 0.5 mL of the concentrated nanocrystal solution was mixed with 9.5 mL of concentrated nitric acid over the period of 3 days. After which 0.5 mL of the digested solution is placed in a 9.5 mL of nanopure-water.

Chemicals and Reagents. All solvents, except deionized water, were purchased from Aldrich (reagent grade) and distilled prior to use. All reactants, including 3-mercaptopropionic acid (MPA), $ZnSO_4$, $MnSO_4$, $Cu(OAc)_2$ and Na_2S, were purchased from Aldrich and used as received.

Syntheses of MPA Capped ZnS:M (M = Cu and Mn) Nanocrystals. To synthesize MPA capped ZnS based nanocrystls, we followed a previously reported aqueous synthesis of mercaptoacetic acid (MAA) capped ZnS:Mn nanocrystals *via* the formation of zinc (II) ion containing complexes as reactive intermediates with slight modifications.[16] A 50 mL aqueous solution of $ZnSO_4 \cdot 5H_2O$ (1.44 g, 5 mmol) was slowly added to a 50 mL aqueous solution containing 5 mmol of MPA and NaOH (0.40 g, 10 mmol) at 5 °C (ice-water bath). The solution was warmed to ambient temperature after 1 hour's stirring. Separate from this, $MnSO_4 \cdot H_2O$ (0.015 g, 0.1 mmol, for ZnS:Mn) or $Cu(OAc)_2$ (0.02 g, 0.1 mmol, for ZnS:Cu) and Na_2S (0.40 g, 5 mmol) were dissolved in 20 mL 0.01 M HCl. This mixture was subsequently transferred to the flask containing the Zn-MPA complex under vigorous stirring. The resulting solution was refluxed for 10 hours. Slow cooling to ambient temperature and the addition of anhydrous ethanol resulted in a yellow-white precipitate at the bottom of the flask. Finally, the obtained solids were separated by centrifuging and decanting the supernatant. The solids were then dried for 24 hours in a vacuum oven. The obtained experimental data are summarized in Table 1.

Photoluminescence (PL) Efficiency Measurements. The PL efficiencies for the ZnS based nanocrystals were measured and calculated by the method previously reported by Williams *et al*.[21] which is to calculate a relative quantum yield by comparing to that of a standard material in literature,[22] 0.1 M solution of quinine sulfate in H_2SO_4 (Fluka) in our case, of which the emission wave length and reported absolute quantum yield are 550 nm and 0.546 (at 22 °C) respectively. In these experiments, the used excitation wavelengths for the standard (quinine sulfate) were obtained from the UV/Vis spectrum from each nanocrystal. The emission spectra for both standard and comparing nanocrystals were recorded at five different concentrations in aqueous solvents. We then plotted a graph of integrated fluorescence intensity versus absorbance for both samples obtained at different concentrations. As a result we were able to obtained straight lines with fairly constant gradients, and their intercepts were at zero. Finally, the relative PL efficiencies were calculated using the following equation:[21]

$$\Phi_x = \Phi_{ST}\left(\frac{Grad_x}{Grad_{ST}}\right)\left(\frac{\eta_x^2}{\eta_{ST}^2}\right)$$

In this equation, Φ represents PL efficiency. The subscript ST and x denote the standard (quinine sulfate) and the

Table 1. Data summary of MPA capped ZnS based nanocrystals

	ZnS-MPA	ZnS:Cu-MPA	ZnS:Mn-MPA
UV/Vis absorption (λ_{max}, nm)	320	320	320
PL emission wavelength (λ_{max}, nm)	440	510	590
PL excitation wavelength (λ_{max}, nm)	317	327	320
PL efficiency (%)	4.38	6.61	7.20
HR-TEM (average particle size, nm)	4.5	4.5	5.0
ICP-AES Amount of dopant ions (%)	N/A	1.75	1.61
FT-IR (frequencies, cm^{-1}) (w = weak, m = moderate, s = strong)	3226(s), 2974(w), 2356(w), 2320(w), 2290(w), 2169(w), 2115(w), 1992(w), 1623(s), 1549(s), 1395(s), 1311(m), 1276(s), 1201(m), 1154(s), 1123(m), 1109(m), 968(m), 939(m), 864(m), 814(w), 759(w), 667(w)	3185(s), 2198(w), 1981(w), 1645(w), 1550(s), 1387(s) 1301(w), 1269(w), 1009(s)	3190(s), 2185(w), 1985(w), 1641(w),1 548(s), 1391(s) 1296(w), 1265(w), 1106(w), 1009(s)

corresponding nanocrystal respectively. In addition, 'Grad' indicates the gradient from the plot of integrated fluorescence intensity versus absorbance, and 'η' represents the refractive index of the solvent, a factor which we eliminated by using the same solvent (water) for both standard and the nanocrystal.

Results and Discussions

The average particle sizes of the ZnS based nanocrystals were measured from the HR-TEM images presented in Figure 1. Even though those images did not clearly show discrete individual particles, we enlarged the images to a maximum and measured about 30 identifiable particles to obtain the average particle size for the ZnS based nanocrystals. In the images, the shapes of the particles are fairly close to the sphere and the measured particle sizes are 4.5 nm (ZnS), 4.5 nm (ZnS:Cu), and 5.0 nm (ZnS:Mn), respectively, which are slightly larger than that for the other ligands (*e.g.*, aminoacids) capped ZnS:Mn nanocrystals (3.3 nm in average).[15] To support our measurements through the TEM images, we also performed Debye-Scherrer calculations. In the figures, small agglomerations between the particles were observed due to the evaporation of the solvents during the sample preparation. However, the appearance of distinct lattice planes in the HR-TEM image with about 3 Å lattice spacing indicate that the obtained solids are made of single crystals rather than poly-crystalline aggregates for all the nanocrystal samples.

Energy dispersive x-ray spectroscopy diagrams (EDXS, in Fig. 2) were also obtained to confirm the elemental compositions of the ZnS based nanocrystals in the solid state. The obtained doping concentration of copper(II) ions in the ZnS:Cu was 0.23 at %, while that of manganese(II) ions in the ZnS:Mn nanocrystal was 1.1 at %. To determine the doping concentration of metal ions more precisely, Inductively Coupled Plasma-Atomic Emission Spectrometry (ICP-AES) analyses were also performed. Three trials of the sample measurements revealed that the average elemental proportions of the Cu^{2+} and Mn^{2+} ions relative to ZnS parent crystal were 1.75 and 1.61 at %, respectively. The intended dopant concentrations in our ZnS based nanocrystals were in the range of 1% to 2%, which had been reported in the literature as the optimum dopant amount for most ZnS based nanocrystals to obtain maximum luminescence.[23]

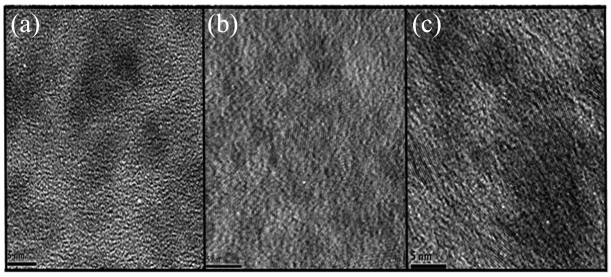

Figure 1. HR-TEM images of: (a) ZnS (b) ZnS:Cu and (c) ZnS:Mn nanocrystals.

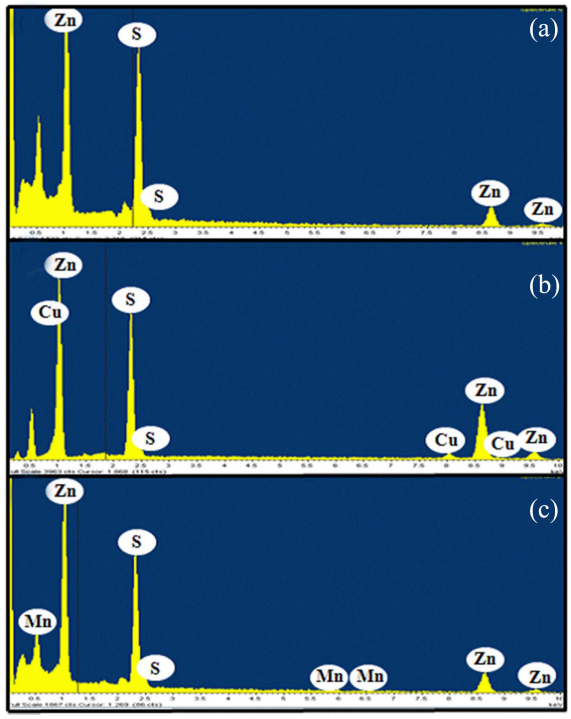

Figure 2. EDXS diagrams of : (a) ZnS (b) ZnS:Cu and (c) ZnS:Mn nanocrystals.

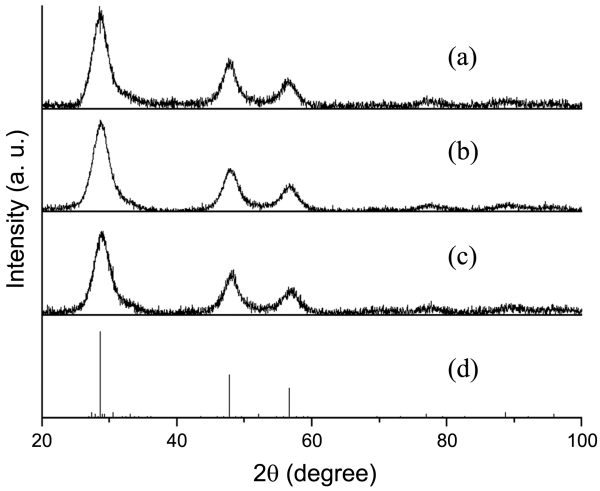

Figure 3. XRD pattern diagrams of : (a) ZnS (b) ZnS:Cu and (c) ZnS:Mn nanocrystals and (d) reference bulk ZnS solid in a wurtzite phase.

As shown in Figure 3, wide-angle x-ray diffraction (XRD) pattern diagrams of the ZnS based nanocrystalline powders were obtained to confirm the formation of ZnS parent crystal lattices. In the diffraction pattern diagrams, the apparent peaks at the (008), (110), and (118) planes for the ZnS based nanocrystal powder samples are identical to those for the reported bulk ZnS solid in a hexagonal wurtzeite crystalline phase (JCPDS 39-1363).[24] In addition, we also performed Debye-Scherrer calculations for ZnS based nanocrystals by using the obtained XRD peaks to compare with the particle size measured from the HR-TEM images.[25] From the measured full width at half maxima (FWHM) of the selected

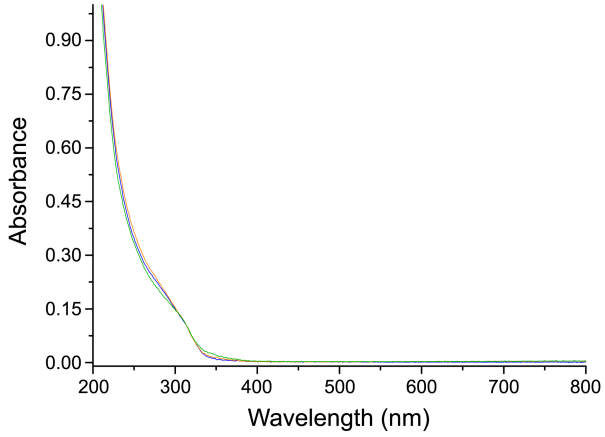

Figure 4. UV-visible absorption spectra of: ZnS (blue), ZnS:Cu (green) and ZnS:Mn (orange) nanocrystals.

XRD peaks, we obtained the calculated average particle sizes for ZnS, ZnS:Cu, and ZnS:Mn nanocrystals, which were 5.6 nm, 7.2 nm, and 6.9 nm respectively.

Figure 4 presents the solution photoluminescence (PL) emission spectra obtained from the ZnS based nanocrystals in aqueous solution, in which broad emission peaks appeared at 440 (ZnS), 510 (ZnS:Cu), and 600 (ZnS:Mn) nm wavelengths. The corresponding emission spectra were obtained by fixing the light source at the maximum absorption wavelengths in the UV-Visible spectra, which were the same at 320 nm for all the nanocrystals as shown in Table 1. The dominant absorption shown in the UV-Vis spectra were probably caused by the fundamental band-to-band absorption in the ZnS host,[26] and the increased band gap of the ZnS-MPA nanocrystal (3.87 eV) compared to that for bulk ZnS solid (3.54 eV) is due to the quantum confinement effect for nanosized materials.[27] The excitation spectra in Figure 5 were also obtained by fixing the light sources at the obtained corresponding emission wave lengths, and the resulting peaks appeared at 317 (ZnS), 327 (ZnS:Cu), and 320 (ZnS:Mn) nm respectively. The observed large Stoke shifts for all the ZnS based nanocrystals, which were in the range of 120 to 280 nm, are among the typical features that appeared in nano-sized semiconductor crystalline materials.[28] These phenomena were mostly due to the recombination of trapped charge carriers as opposed to free carriers. The trapping of the charge carriers occurs at surface defects that lie between the band gap states.[29] The surface defects on the ZnS based nanocrystals probably resulted from incomplete capping by the surfactant MPA molecules, or from the zinc metal cation or sulfide anion vacancy on the surface of the crystal lattice.

Synthesis of the ZnS nanocrystal using different surfactants has been reported by Palve *et al.*[30] The authors obtained ZnS nanocrystal by pyrolysis (515 C) of various Zn and S containing organometallic precursor complexes. Usually, ZnS exists in one of the two crystalline phases, *i.e.* cubic zinc blende (or sphalerite) or hexagonal wurtzite. They showed that choosing a certain precursor can direct the formation of a certain crystalline phase; for example, they obtained a cubic phase ZnS nanocrystal by using the $[Zn(cinnamtscz)_2]$ precursor complex, where the cinnamtscz represents a cinnamaldehydethiosemicarbazone ligand. However, a hexagonal wurtzite ZnS nanocrystal was obtained from different $[Zn(cinnamtsczH)_2]Cl_2$ precursor complexes. The obtained UV-blue light emissions with wavelengths of 326 nm (cubic ZnS) and 368 nm (wurtzite ZnS), which showed significantly blue shifted (UV-Blue) emissions from our hexagonal wurtzite ZnS-MPA (440 nm) nanocrystals. It is known that having more surface defects such as zinc ion vacancy on the surface of ZnS nanocrystal induces stronger emission of blue light.[31] Therefore, we can conclude that the MPA ligand creates more crystal defects than the cinnamtscz ligand during the nanocrystal formation process, and is ironically more important to obtain bright blue color emission from the ZnS nanocrystal.

The green light emission from ZnS:Cu solid has been reported by Peng *et al.*[32] The green light emission at 510 nm arises from the recombination between the shallow donor level created by a sulfur vacancy and the t_2 level of Cu^{2+} ions. It is also known that doping concentration of Cu^{2+} plays a critical role for the luminescence property of the ZnS:Cu nanocrystal. Increasing Cu concentration can push the t_2 level of Cu^{2+} ions farther away from the valence band; therefore, the emission was significantly quenched when the dopant ion concentration reached over 2 at % against the ZnS host. In a particular case, red-orange light emission from the ZnS:Cu nanocrystal was reported by Bol et al;[33] however, we did not observe this phenomenon with our ZnS:Cu-MPA nanocrystal.

In the ZnS:Mn-MPA nanocrystal, the yellow-orange light emission at 600 nm is attributed to the $^4T_1 - {}^6A_1$ transition of Mn^{2+} ions.[34] In the luminescence pathway, if the surface defect states are located close to the conduction band, the direct energy transfer from the ZnS host to the Mn^{2+} activator

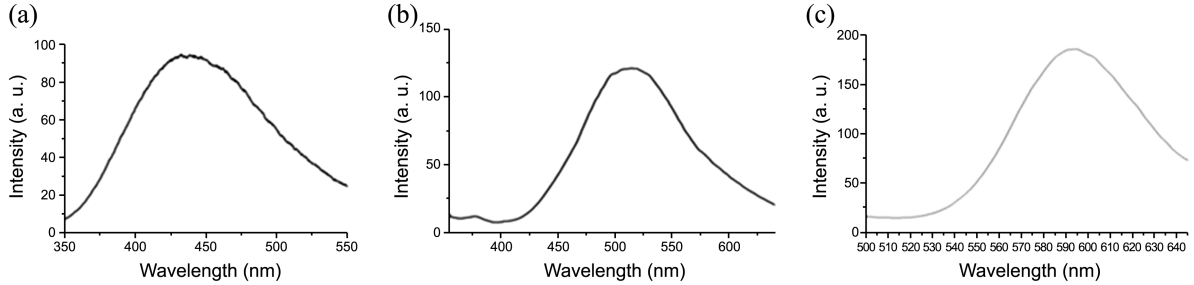

Figure 5. PL emission spectra of: (a) ZnS (b) ZnS:Cu and (c) ZnS:Mn nanocrystals.

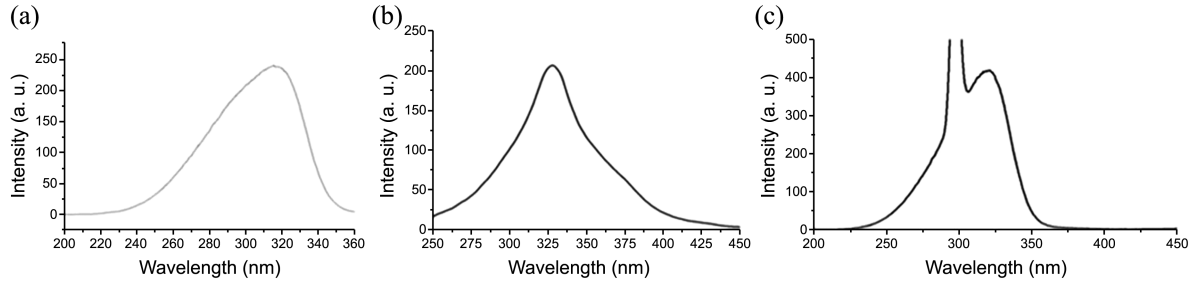

Figure 6. PL excitation spectra of: (a) ZnS (b) ZnS:Cu and (c) ZnS:Mn nanocrystals.

is significantly interrupted, which can cause weakening in the orange emission as well as enlarging of the Stokes shift.[35] In a special case, a direct white light emission from a manganese ion doped ZnS nanocrystal was observed by using 8-hydroxyquinoline-5-sulfonic acid (HQS) as the surfactant.[36] The ZnS:Mn-HQS showed two emission PL peaks at 475 nm (blue) and 600 nm (yellow-orange) wavelengths. The blue emission at 475 nm from the ZnS:Mn-HQS was described as a result of the incomplete energy transfer between the ZnS lattice and the dopant ion due to the presence of both interstitials and vacancies of zinc or sulfide ions in the ZnS lattice.[37] However, we were not able to observe such phenomenon from our ZnS:Mn-MPA nanocrystal, which also indicates the surface capping ligand dependent properties of ZnS based nanocrystals.

As described in the previous experimental section, the PL efficiencies for the ZnS based nanocrystals were measured and calculated by following the same method as that reported by Williams *et al.*[20] to calculate the relative quantum yield by comparing to a standard material in the literature[21] (0.1 M solution of quinine sulfate in H_2SO_4 (Fluka) in our case), of which the emission wavelength and reported absolute quantum yield are 550-600 nm and 0.546 (at 22 °C), respectively. The excitation wavelength (320 nm) used for the standard (quinine sulfate) solution was obtained from the UV/Vis spectra for the ZnS based nanocrystals. As a result, the calculated relative PL efficiencies for the ZnS based nanocrystals were 4.38% (ZnS), 6.61% (ZnS:Cu), and 7.20% (ZnS:Mn), respectively . The obtained PL efficiencies of the ZnS based nanocrystals are quite similar to those obtained from other ligands (*i.e.* aminoacids and MAA) capped ZnS:Mn nanocystals.[14-16]

In Figure 6, the presented light scattering pictures were taken by exposing the ZnS based nanocrystals containing aqueous colloidal solutions to 325 nm He/Cd laser light of which the emission wavelength is close to the excitation wavelengths of the ZnS based nanocrystals. The pictures show bright light scattering of the blue (ZnS), green (ZnS:Cu), and yellow-orange (ZnS:Mn) colors of the ZnS based nanocrystals containing colloidal solutions. In addition, Figure 7 shows a white light scattering from a mixture solution of the three ZnS based nanocrystals, with the optimum molar ratio of 20 (ZnS):1 (ZnS:Cu):2 (ZnS:Mn). The molar concentrations of the nanocrystals in aqueous solution, represented as [ZnS:M], were determined by elemental analysis by ICP-AES measurements as described in the literature.[38] The obtained Zn and dopant metal ion concentrations were combined and converted into the nanocrystal particle concentration, assuming that the nanocrystal particle holds the same density as its bulk material. The exceedingly high mixing ratio of the blue ZnS-MPA nanoparticle required to produce white light emission would be expected since scattering of blue light by the nanoparticles is much greater than that of green or yellow-orange lights when the diameters of the present particles are similar.[39] In other literature, it has been reported that one of the major causes of efficiency loss (up to 70%) in a white LED is scattering of the blue excitation light by the phosphor particles.[40] The CIE chromaticity diagram presented in Figure 7 shows the positions of the color coordinates for each ZnS based nanocrystal and the mixture. The obtained color coordinate was (x = 0.31, y = 0.34) for the mixture of the ZnS based nanocrystals, which indicates very close to a perfect white color combination. For other ligands capped ZnS based nanocrystals, it has been reported that the emitting colors were slightly changed by varying the concentration of the dopant ions[31,34]; however, we did not observe such changes for our MPA capped ZnS based nanocrystals. In addition, the measured color temperature for the white light emitting mixture was 5527 K, which is very close to the daylight (white light) balanced photographic film standard of 5500 K.[41]

Finally, the surface capping molecules (MPA) were

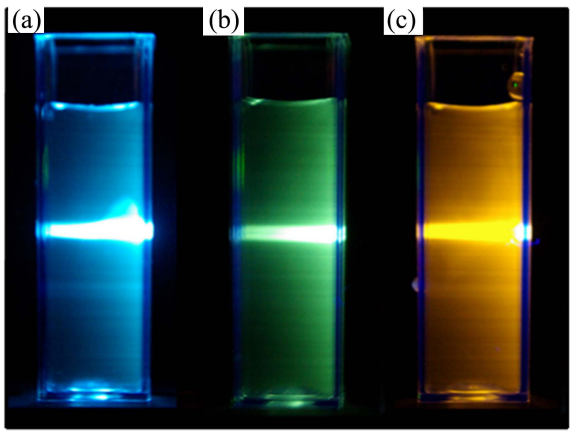

Figure 7. Laser light scattering images of (a) ZnS (blue), (b) ZnS:Cu (green), (c) ZnS:Mn (yellow-orange) nanocrystals.

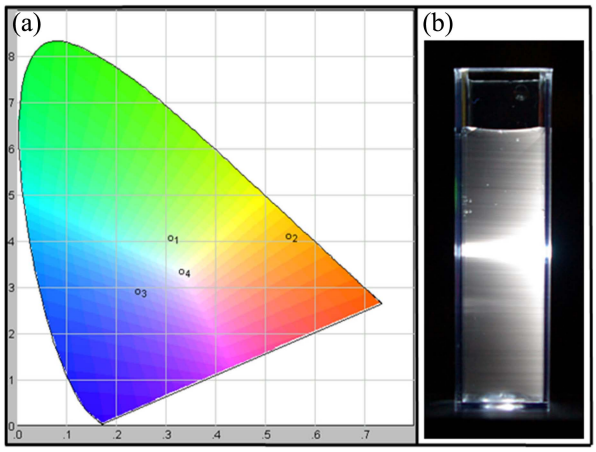

Figure 8. CIE diagram and Laser light scattering image of the mixed ZnS based nanocrystals. (color coordinates: O_1 (ZnS), O_2 (ZnS:Cu), O_3 (ZnS:Mn), and O_4 (mixture)).

characterized by FT-IR and FT-Raman spectroscopy. Figure 8 shows FT-IR spectra of ZnS-MPA and uncoordinated free MPA molecule for a comparing reference material. In fact those obtained spectra were very similar to that for mercaptoacetic acid (MAA) capped ZnS:Mn nanocrystal 16 since the only difference between MPA and MAA is one methyl group moiety in the carbon back chain. In addition, FT-IR spectra obtained from the three ZnS based nanocrystals were almost identical to each other, which are probably caused by having similar reduced mass and binding affinity for Zn-S, Cu-S and Mn-S moieties.[42] Therefore, we presented only ZnS-MPA case in this figure to characterize the MPA ligand boud on the surface of the nanocrystals. All the obtained FT-IR peak data are listed in Table 1. The overall spectrum of the ZnS-MPA nanoparticles was found to differ somewhat to that obtained by the free MPA molecule. The absence of the S-H stretch at 2570 cm^{-1} in ZnS-MPA suggests that MPA exists as a thiolate on the nanocrystal surface.[43] In addition, due to the deprotonation and coordination with the heavier metal ions of the carboxylic acid group, the C=O stretching band of neat MPA at 1692

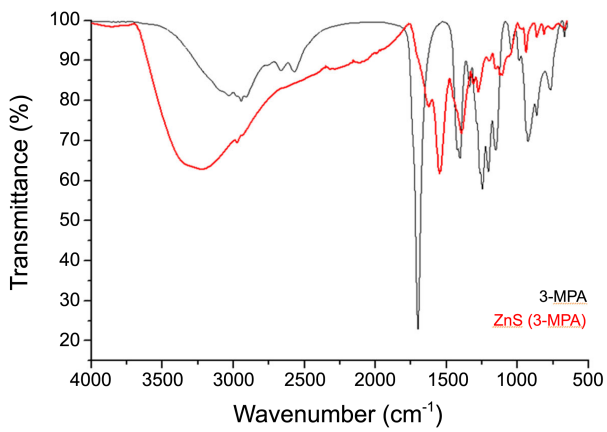

Figure 9. FT-IR spectra of ZnS-MPA (red) and free MPA solid (black): peaks are listed in Table 1.

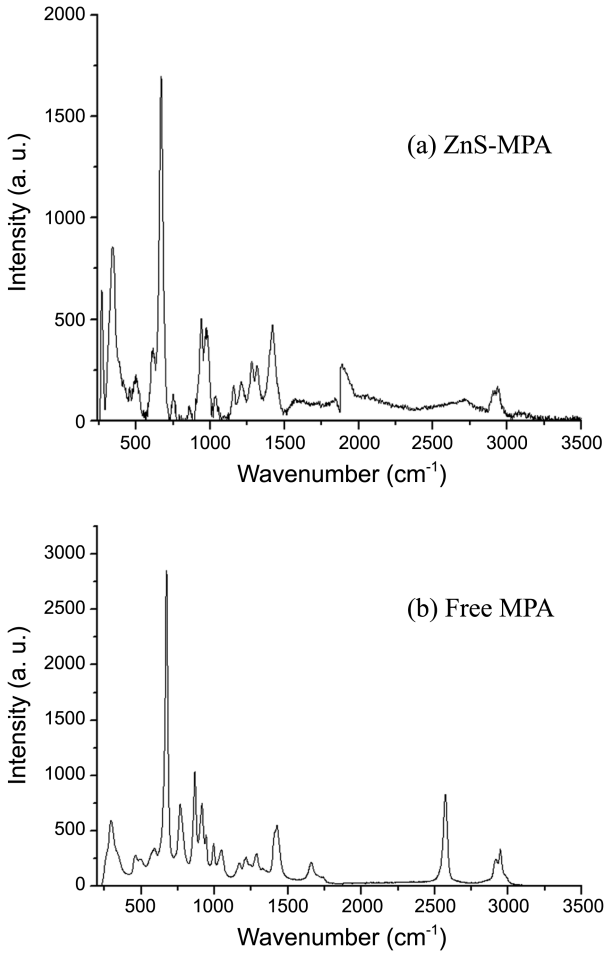

Figure 10. FT-Raman spectra of (a) ZnS-MPA nanocrystal and (b) neat (free) MPA : peaks are listed in Table 2.

cm^{-1} shifted and separated to an antisymmetric OCO stretch at 1549 cm^{-1} and a symmetric OCO stretch at 1395 cm^{-1} for ZnS-MPA nanocrystals.[44] This phenomenon was also observed for a metal ion coordinated MPA molecule such as Na-MPA salt.[45] To remove any uncoordinated or unreacted MPA molecules, the centrifuged white solids were rapidly washed several times with cold alcohol/water mixture solutions. As a result, the peaks that resulted from the free MPA molecules were removed from the presented FT-IR spectra. FT-Raman spectrum of ZnS-MPA nanocrystal was presented in Figure 9. The obtained peaks are listed in Table 2 and compared with those of neat MPA and MPA coordinated silver nanoparticles (Ag-MPA).[46] The overall FT-Raman spectrum of the ZnS:Mn-MPA nanoparticles was found to closely resemble that of FT-IR spectrum in Figure 8 except high frequency region around 3226 cm^{-1} and low frequency regions. As shown in FT-IR spectrum, the absence of S-H stretch at 2576 cm^{-1} also supprots that MPA exists as a thiolate on the nanocrystal surface. In addition, due to deprotonation of carboxylic acid group, the C=O stretching band of neat MPA at 1662 cm^{-1} switched to an antisymmetric OCO stretch at 1637 cm^{-1} and a symmetric OCO stretch at 1419 cm^{-1}. Data analyses of the low frequency region are rather challenging since the binding between ZnS and MPA restrict low fre-

Table 2. FT-Raman data of MPA capped ZnS nanocrystal (wave numbers in cm^{-1})

Neat MPA	Ag-MPA (ref. 46)	ZnS-MPA	Assignments (ref. 46)
293(w)	300(vw)		δ(SCC)
		337 (m)	Zn-S phonon
462(vw)	480(w)		δ(CCO)/ρ(OCO)
593(vw)	608(vw)	504(w)	δ(CCO)/ω(OCO)
	668(sh)		δ(OCO)
674(s)	684(s)		$\nu(CS)_G$
766(m)	760(w)	748(s)	$\nu(CS)_T$
	851(w)		$\rho(CH_2)$
867(m)			δ(SH)
914(m)	937(s)	939 (w)	ν(C-COO)
943(w)	950(sh)		$\rho(CH_2)$
995(w)			ν(CC)
1047(w)	1020(w)	1035(m)	ν(CC)
1170(vw)		1158(m)	$tw(CH_2)$
1214(vw)	1220(w)	1215 (m)	$tw(CH_2)$
1293(w)	1277(w)	1279(w)	$\omega(CH_2)$
1293(w)			ν(CO)+δ(OH)
1331(vw)	1303(m)	1317(m)	$\omega(CH_2)$
	1406(m)	1419(w)	ν_s(OCO)
1416(sh)			$\delta(CH_2)$/ν(CO)+δ(OH)
1430(m)	1440(w)	1426(m)	$\delta(CH_2)$
	1560(vw)		ν_{as}(OCO)
1662(m)		1657(m)	ν(C=O)
2576(vs)			ν(SH)
2922(s)	2926(vs)	2934(w)	$\nu_s(CH_2)$
2950(vs)			$\nu_{as}(CH_2)$

quency bending, twisting, and torsional motions. As a result, these bands are considerably down shifted compared with those of free MPA molecule. According to the literature, the peak appeared at 337 cm^{-1} can be assigned to transverse and longitudinal optical phonon of Zn-S lattice.[47]

Conclusion

In summary, we have successfully synthesized three different ZnS based nanocrystals that have the same parent: ZnS, ZnS:Cu and ZnS:Mn. The nanocrystals were optically characterized by UV/Vis and room-temperature PL spectroscopy. The further physical analyses were performed by XRD, HR-TEM, EDXS, and ICP-AES. The PL spectra showed emission peaks at 440 (ZnS), 510 (ZnS:Cu) and 600 (ZnS:Mn) nm, and white light was produced by mixing these nanocrystals in aqueous solution. While the emitting lights from the nanocrystals were not perfect complementary color combinations to each other, we were able to obtain white-color emission by mixing the three nanophosphors at a proper ratio. In this lab, further application studies such as fabrication of electronic illumination devices such as white QD-LEDs using those ZnS based nanocrystasl are in progress.

Acknowledgments. The present research was supported by the Research Fund of Dankook University in 2011.

References

1. Alivisatos, P. *J. Phys. Chem.* **1996**, *100*, 13226.
2. Murray, C. B.; Norris, D. J.; Bawendi, M. G. *J. Am. Chem. Soc.* **1993**, *115*, 8706.
3. Jaiswal, J. K.; Mattoussi, H.; Mauro, J. M.; Simon, S. M. *Nature Biotechnol.* **2002**, *21*, 47.
4. Revaprasadu, N.; Malik, M. A.; O'Brien, P. *J. Mater. Chem.* **1998**, *8*, 1885.
5. Hines, M. A.; Guyot-Sionnest, P. *J. Phys. Chem. B* **1998**, *102*, 3655.
6. Hwang, J. M.; Oh, M. O.; Kim, I.; Lee, J. K.; Ha, C.-S. *Curr. Appl. Phys.* **2005**, *5*, 31.
7. Yu, S. H.; Wu, Y. S.; Yang, *J. Chem. Mater.* **1998**, *9*, 2312.
8. Brus, L. E. *Appl. Phys. A: Solid Surf.* **1991**, *53*, 465.
9. Dabbousi, B. O.; Bawendi, M. G.; Onitsuka, B. O.; Rubner, M. F. *Appl. Phys. Lett.* **1995**, *66*, 11.
10. Gerion, D.; Pinaud, F.; Williams, S. C.; Parak, W. J.; Zanchet, D.; Weiss, S.; Alivisatos, A. P. *J. Phys. Chem. B* **2001**, *195*, 8861.
11. Jun, Y. W.; Jang, J. T.; Cheon, J. W. *Bull. Korean Chem. Soc.* **2006**, *27*, 961.
12. Jaiswal, J. K.; Mattoussi, H.; Mauro, J. M.; Simon, S. M. *Nature Biotechnol.* **2002**, *21*, 47.
13. Heath, J. R. *Acc. Chem. Res*. **1999**, 32.
14. Hwang, C. S.; Lee, N. R.; Kim, Y. A.; Park, Y. B. *Bull. Korean Chem. Soc.* **2006**, *27*, 1809.
15. Lee, J. H.; Kim, Y. A.; Kim, K.; Huh, Y. D.; Hyun, J. W.; Kim, H. S.; Noh, S. J.; Hwang, C. S. *Bull. Korean Chem. Soc.* **2007**, *28*, 1091.
16. Kim, J. E.; Hwang, C. S.; Yoon, S. *Bull. Korean Chem. Soc*. **2008**, *29*, 1247.
17. Huang, J.; Li, G.; Wu, E.; Xu, Q.; Yang, Y. *Adv. Mater.* **2006**, *18*, 114.
18. Tamura, T.; Setomote, T.; Taguchi, T. *J. Lumin*. **2000**, *87*, 1180.
19. Bowers, M. J.; McBride, J. R.; Rosental, S. J. *J. Am. Chem. Soc.* **2005**, *127*, 15378.
20. Lee, S. M.; Hwang, C. S. *Bull. Korean Chem. Soc*. **2013**, *34*, 321.
21. Rhys-Williams, A. T.; Winfield, S. A.; Miller, J. N. *Analyst* **1983**, *108*, 1067.
22. Melhuish, W. H. *J. Phys. Chem*. **1961**, *65*, 229.
23. Yi, G.; Sun, B.; Yang, F.; Chen, D. *J. Mater. Chem*. **2001**, *11*, 2928.
24. *International Union of Crystallography in International Tables for X-ray Crystallography, Part III*; Dordrecht, Netherlands, 1985; p 318.
25. Kushida, T.; Tanaka, Y.; Oka, Y. *Solid State Commun*. **1974**, *14*, 617.
26. Hasse, M. A.; Qui, J.; DePuydt, J. M.; Cheng, H. *Appl. Phys. Lett.* **1991**, *59*, 1272.
27. Lippens, P. E.; Lannoo, M. *Phys. Rev. B* **1989**, *39*, 10935.
28. Tata, M.; Banerjee, S.; John, V. T.; Waguespack, Y.; Mcpherson, G. *Colloids Surf. A* **1997**, *127*, 39.
29. Zhuang, J.; Zhang, X.; Wang, G.; Li, D.; Yang, W.; Li, T. *J. Mater. Chem*. **2003**, *13*, 1853.
30. Palve, A. M.; Garje, S. S. *Bull. Mater. Sci*. **2011**, *34*, 667.
31. Goswami, B.; Pal, S.; Sarkar, P. *J. Phys. Chem. C* **2008**, *112*, 11630.
32. Peng, W. Q.; Cong, G. W.; Qu, S, C.; Wang, Z. G. *Opt. Mater.* **2006**, *29*, 313.
33. Bol, A. A.; Frewerda, J.; Bergwerff, J. A.; Meijerink, A. *J. Lumin*. **2002**, *99*, 325.
34. Chen, W.; Su, F.; Li, G.; Joly, A. G.; Malm, J.-O.; Bovin, J.-O. *J. Appl. Phys*. **2002**, *92*, 1950.
35. Dong, B.; Cao, L.; Su, G.; Liu, W.; Zhai, H. *J. Alloys Compd.* **2010**, *429*, 363.
36. Lü, X.; Yang, J.; Fu, Y.; Liu, Q.; Qi, B.; Lü, C.; Su, Z. *Nanotech*.

2010, *21*, 115702.
37. Sarkar, R.; Tiwary, C. S.; Kumbhakar, P.; Basu, S.; Mitra, A. K. *Physica E* **2008**, *40*, 3115.
38. Yu, W. W.; Qu, L.; Guo, W.; Peng, X. *Chem. Mater.* **2003**, *15*, 2854.
39. Dichburrn, R. W. *Light*, 2nd Ed.; Blackie and Sons: London, 1963; p 582.
40. Kasuya, R.; Kawano, A.; Isobe, T. *Appl. Phys. Lett.* **2007**, *91*, 111916.
41. George, C. *Mastering Digital Flash Photography: The Complete Reference Guide*; Sterling Publishing Company: 2008; p 11.
42. Brisdon, A. K. *Inorganic Spectroscopic Methods*; Oxford Univ. Press: 1998; chap. 2, p 11.
43. Pandiarajan, S.; Umadevi, M.; Rajaran, R. K.; Ramakrishinan, V. *J. Spectrochim. Acta A* **2005**, *62*, 630.
44. Moszczenski, C. W.; Hooper, R. J. *Inorg. Chim. Acta* **1983**, *70*, 71.
45. Ito, K.; Bernstein, H. J. *Can. J. Chem.* **1956**, *34*, 170.
46. Castro, J. L.; Lopez-Ramirez, M. R.; Arenas, J. F.; Otero, J. C. *J. Raman Spectrosc.* **2004**, *35*, 997.
47. Schneider, J.; Kirby, R. D. *Phys. Rev. B* **1972**, *6*, 1290.